CSCE Annual Conference

Growing with youth – Croître avec les jeunes

Laval (Greater Montreal)

June 12 - 15, 2019

LOCAL BUCKLING ANALYSIS OF MULTISIDED STEEL TUBE SECTIONS

Zannatul Mawa Dalia[1], and Anjan K Bhowmick[2]

[1] Graduate Research Assistant, Concordia University, Canada

[2] Associate Professor, Department of Building Civil and Environmental Engineering, Concordia University, Canada

Abstract: Multisided steel tubular sections are commonly used in many structures such as light posts, road signpost, transmission and telecommunication towers etc. These sections are generally subjected to axial compression and bending. From the design point of view, it is very important to make sure that these thin-walled sections do not buckle locally before yielding. While current AASHTO has provided slenderness limits to check for local buckling of eight, twelve and sixteen sided polygonal steel sections, very limited study has been conducted to evaluate these slenderness limits. This paper presents a finite element (FE) analysis based study of local buckling of multisided steel tubular sections. A nonlinear finite element model which includes both material and geometric nonlinearities is developed for this study. The finite element model is validated against experimental results from four stub columns of three different cross sections (i.e. Octagonal, Dodecagonal, and Hexadecagonal) tested under concentric compression. The validated finite element model is then used to analyze a series of multisided steel tubular sections under axial compression and pure bending. Three different geometry, namely, eight, twelve and sixteen sided polygonal sections are considered. Both linear buckling and nonlinear static analyses are conducted using ABAQUS. Results from FE analyses are compared with limits specified in different standards.

1 INTRODUCTION

Thin-walled multisided tubular steel sections are commonly used as light post, signposts, transmission, and telecommunication towers. Because of a smaller thickness, these thin-walled structures have a tendency to buckle locally if proper slenderness ratio is not maintained. This type of sections are generally subjected to both axial compression and bending. An adequate understanding of local buckling of the thin-walled multisided tube is necessary to ensure the effective service of these structures.

Elastic buckling stress of thin-walled tubular multisided sections can be determined by considering them as an assembly of restrained plates. Using elastic analysis, elastic critical buckling stress of multisided steel tubular sections can be found from following equation 1 (Timoshenko 1961).

$$[1]\ \sigma cr = \frac{k\pi^2 E}{12(1-\nu^2)\left(\frac{b}{t}\right)^2}$$

where k is called the plate buckling coefficient determined by theoretical critical-load analysis and is a function of plate geometry and boundary conditions. E, ν, b and t are the modulus of elasticity, poison's ratio, plate width, and thickness, respectively. In case of the simply supported plate, the k value of 4 can be used. Several studies have been undertaken to find values of k for different geometry, loading, and support conditions.

Teng et al. (1999) investigated the elastic local buckling behavior of polygonal columns subjected to either axial compression or uniform bending. They have investigated the variation of elastic plate buckling coefficient k with a number of sides of section and nature of loading. K values are presented for a variety of width-thickness ratios. Among the square, pentagonal, hexagonal, heptagonal and octagonal shape; the pentagonal shape was found to be strongest under axial compression or bending. It was also reported that sections with an odd number of sides have higher buckling capacity as compared to sections having even number of sides (Teng et al. 1999).

Aoki et al. (1991) studied the local buckling behavior of regular polygonal, short length steel columns. It was mentioned that polygonal sections having more faces among the thin-walled members with the same cross-sectional area, may become advantageous for local buckling strength. Equation 2 shows the empirical design formula to predict the local buckling strength of the polygonal section columns (Aoki et al. 1991).

$$[2]\ \frac{\sigma \max}{\sigma y} = 1.35 - 0.55\,\mathrm{R} \qquad (\mathrm{R} > 0.636)$$

where R is a width-thickness parameter of plate elements which can be obtained as $R=\sqrt{(\sigma_y/\sigma_{cr})}$, where σ_{cr} is elastic critical buckling stress with k=4.

The elasto-plastic local buckling behavior of the polygonal thin-walled steel sections was investigated by Migita et al. (1997). It was found that, in spite of the various number of sides, the difference in the average buckling stresses is small for the same value of R, where R is a width-thickness parameter of plate elements. Based on the analytical and experimental results, two formulae were proposed to estimate the local buckling strength of polygonal sections (Migita et al.1997).

Godat et al. (2011) investigated the local buckling behavior of polygonal tubular sections having 8, 12 and 16 number of sides. It was reported that thin-walled polygonal tubular sections having the same cross-sectional area and smaller plate slenderness ration may become advantageous. Furthermore, it was found that the number of faces was not influencing parameter in local buckling capacity when plate width to thickness ratio is kept constant. It was observed that the ASCE (ASCE/SEI-48-05 2006) tends to overestimate the experimental results for plate slenderness parameter lower than 1.5. The Eurocode 3 (EN 1-1, 2005, EN 1-3, 2006, EN 1-5, 2006) overestimates greatly the capacity for high width-to-thickness ratios. Design equation for critical buckling capacity has been proposed for the tubular polygonal section with a different form of cross-sections (Godat et al. 2011).

Current AASHTO (AASHTO 2015) has provided width-thickness limits for eight, twelve and sixteen sided polygonal steel sections. However, very limited study has been conducted to evaluate these limits. ASCE (ASCE/SEI-48-11 2011) provides design equations for local buckling capacity of eight, twelve and sixteen sided polygonal steel sections of transmission line. Eurocode 3 (EN 1-1, 2005, EN 1-3, 2006, EN 1-5, 2006) has design equation for plate elements. In this study, multisided steel tubular section has been considered as a collection of individual longitudinal plate strip to find the resistance using Eurocode 3. The objective of this study is to observe the local buckling behavior of multisided steel tubular section under compression and pure bending by developing Finite Element Models (FEM). Finite Element Models have been compared with existing codes. Three different geometry, namely, eight, twelve and sixteen sided polygonal sections are considered. The behavior of other Hollow Structural Sections is out of the scope of this paper.

2 FINITE ELEMENT MODELING

2.1 Elements and Properties

A nonlinear finite element model is developed using ABAQUS software. Both material and geometric nonlinearities have been considered in modelling. Thin-walled members of three different cross-sections (i.e. Octagonal, Dodecagonal, and Hexadecagonal) have been modelled using 4-node shell elements with reduced integration (S4R from ABAQUS element library). To apply the compressive load, a top plate was modelled with 10-node tetrahedral element C3D10 (ABAQUS 2014).

2.2 Boundary Conditions

All the specimens were kept simply supported along the reaction surfaces but effectively restrained against the radial movement.

1. Bottom end was restrained against X, Y and Z- axis deflection (U1= U2= U3= 0) and rotation about Z-axis (UR3=0). Rotation about X and Y-axis was kept unrestrained.
2. Top end was restrained against X and Y- axis deflection (U1= U2= 0) and rotation about Z-axis (UR3=0). Rotation about X and Y-axis and deflection in Z-axis were kept unrestrained.

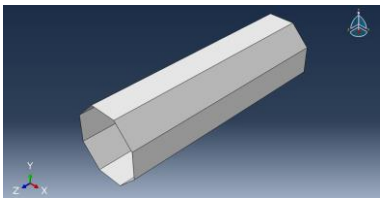

Figure 1: Octagonal Hollow Section

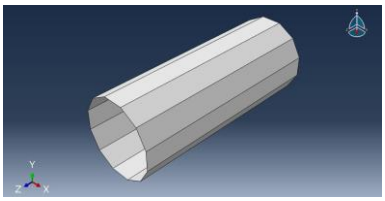

Figure 2: Dodecagonal Hollow Section

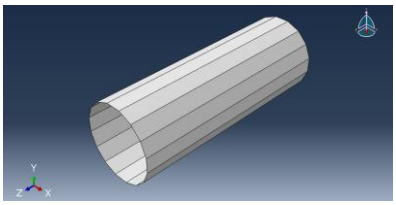

Figure 3: Hexadecagonal Hollow Section

2.3 Analysis Type

Both elastic buckling analysis and nonlinear static analysis were performed to estimate the critical buckling load and flexural capacity of the multi-sided tube. First, an eigenvalue analysis was performed using the linear perturbation buckling analysis. From the eigenvalue analysis, eigenvalues of corresponding eigenmodes were extracted. In this study, three eigenvalues for each member were obtained.

Finally, Static RIKS method (ABAQUS 2014) was used to conduct the nonlinear buckling analysis. RIKS method is suitable for predicting buckling, post-buckling, or collapse of certain types of structures. RIKS method is based on Arc-length method and a form of Newton-Raphson iteration method. It uses an additional unknown, named load proportionality factor. RIKS method provides solutions for load and displacement simultaneously. From the nonlinear buckling analysis, maximum Load Proportionality Factor (LPF) was extracted to estimate the critical buckling load. All the finite element results presented in this paper is from nonlinear static analysis.

2.4 Load Application

Finite element models were analyzed for axial compression and pure bending. To simulate the practical condition, the load was applied through a solid top plate. The uniformly distributed load was applied over the top surface of the top plate. To transfer the load from the top plate to the hollow column, tie constraint was introduced between the top surface of the plate and the top nodes of the hollow column. The load was applied in the negative Z-direction to create a compressive load to the hollow column. A constant bending moment along the length of the member was applied about X-axis. To apply moment, two reference points were created at the center of the hollow section at both ends of the member.

2.5 Geometric Imperfection

Geometric imperfection was applied to trigger the buckling of the models. An imperfection value of 20% of the thickness of the specimen was used for all the models. Since lowest eigenvalue refers to the load which initiates the buckling of a structure, geometric imperfection has been applied to the buckling mode obtained from the lowest eigenvalue from eigenvalue analysis (Trahair 1993).

3 VALIDATION OF FINITE ELEMENT MODEL

The finite element model is validated against the experiment conducted by Godat et al. (2011). Four stub columns of three different cross sections (i.e. Octagonal, Dodecagonal, and Hexadecagonal) were tested under concentric compression. Columns were simply supported and 780mm long. To simulate the

experimental results, all the geometric and mechanical properties of specimens were kept the same in EFM as the experiment. Both linear and nonlinear buckling analysis has been performed to estimate the critical buckling load. Imperfection values that were measured in the experimental results have been introduced in the first mode of buckling. Table 1 shows number of faces (n), plate thickness (t), width of plate (b), tensile yield stress (F_y), Modulus of Elasticity (E), yield strain (ε_y), ultimate strain (ε_u), critical buckling loads from finite element models (P_{FEM}) for nonlinear analysis and experiment ($P_{Experiment}$) for the validated models.

Table 1: Geometric and Mechanical Properties of Validated Specimen

Specimen	n	t (mm)	b (mm)	Fy (Mpa)	E (GPa)	ε_y X10^-3	ε_u (%)	P_{FEM} (KN)	$P_{Experiment}$ (KN)	% Difference
OCT-1-A	8	1.897	95	279	200	1.4	0.26	324.7	327	0.7
DODE-2-A	12	1.897	75	305	218	1.4	0.25	462.8	515	10
HEXA-1-A	16	1.519	52	277	199	1.4	0.26	315.4	317	0.5
HEXA-4-A	16	1.897	60	302	200	1.5	0.26	502.3	508	1.1

4 MULTISIDED TUBE UNDER AXIAL COMPRESSION AND BENDING

4.1 Analysis of Multisided tube for axial compression

The validated FE model has been used to perform more analysis with different width-thickness ratios (b/t). Thirteen models of 780mm length have been developed to see the effect of axial compression on multisided steel sections. For all the models, Modulus of elasticity, E=200Gpa, Yield Stress, F_y=300Mpa, poisons' ratio, υ =0.3 and ε_u= 0.026 was considered. Table 2 shows the results of nonlinear analysis of models locally buckled under axial compression. The notations A and F_{cr} indicate the cross-sectional area and critical buckling stress respectively.

Table 2: Finite Element Results for Axial Compression

Specimen	n	b (mm)	t (mm)	P_{FEM} (KN)	A (mm^2)	F_{cr} (Mpa)
OCTA-1	8	95	1.897	373.3	1556	239.9
OCTA-2	8	75	1.367	202.7	880	230.3
OCTA-3	8	95	1.5	233.6	1207	193.5
OCTA-4	8	95	0.7	69.9	547	128.0
OCTA-5	8	95	0.93	107.7	733	147.0
DODE-1	12	76	1.367	301.1	1307	230.4
DODE-2	12	75	1.897	471.0	1814	259.6
DODE-3	12	76	1	164.5	941	174.8
DODE-4	12	76	1.3	256.7	1235	207.9
HEXA-1	16	52	1.519	383.7	1333	287.9
HEXA-2	16	60	1.897	557.0	1918	290.4
HEXA-3	16	60	1.5	397.5	1504	264.2
HEXA-4	16	60	0.9	183.1	887	206.4

4.2 Analysis of Multisided tube for Pure Bending

More analysis was conducted on multisided tube members for pure bending. Twenty-two (22) models were developed in ABAQUS. Among these 22 models, 13 were compact and 9 were non-compact sections. Each model had a length of 1500mm. For all models, same material properties were used (i.e. E=200GPa, F_y= 300 MPa, Ultimate stress, F_u=410MPa and ε_u=0.029). Each model was analyzed for both linear and nonlinear analysis (RIKS method) to find the Critical value of bending moment. Moreover, AASHTO provides equations to estimate the critical moment. Table 3 shows bending strength (M) of multisided steel sections according to AASHTO (AASHTO 2015). In Table 3, plastic moment and plastic section modulus have been denoted by M_p and Z_x respectively.

Table 3: Bending Strength of Multisided Steel Sections According to AASHTO

Shape	Compact	Non-compact
Hexadecagonal	$\mathrm{M} = \mathrm{Mp} = \mathrm{Zx} \times \mathrm{Fy}$	$M = Mp[2.59 - \frac{1.43\left(\frac{b}{t}\right)}{\sqrt{E/Fy}}]$
Dodecagonal	$\mathrm{M} = \mathrm{Mp} = \mathrm{Zx} \times \mathrm{Fy}$	$M = Mp[1.77 - \frac{0.69\left(\frac{b}{t}\right)}{\sqrt{E/Fy}}]$
Octagonal	$\mathrm{M} = \mathrm{Mp} = \mathrm{Zx} \times \mathrm{Fy}$	$M = Mp[1.5 - \frac{0.45\left(\frac{b}{t}\right)}{\sqrt{E/Fy}}]$

For each section, bending strength was calculated according to AASHTO and then compared with FEM results of nonlinear analysis. All the multisided tubular sections were locally buckled. Table 4 and Table 5 show the geometric properties and bending strength according to the nonlinear analysis of FEM (M_{FEA}) and AASHTO (M_{AASHTO}). In Tables 4 and 5, λ' and λ_r indicates width-thickness ratio for compact and non-compact limits respectively as per AASHTO. The FE results will be discussed in the next section.

Table 4 Geometric Properties of Compact Sections and FEM results

Specimen	n	b (mm)	t (mm)	λ'	b/t	M_{AASHTO} (KN-m)	M_{FEM} (KN-m)	% Difference
OCT-1-B	8	100	4.5	28.92	22.22	107.3	114.4	6.6
OCT-2-B	8	100	3.6	28.92	27.78	81.0	78.6	3.0
OCT-3-B	8	100	3.8	28.92	26.32	86.6	86.2	0.5
OCT-4-B	8	100	4	28.92	25.00	92.4	93.5	1.3
OCT-5-B	8	100	3.46	28.92	28.90	77.1	74.2	3.7
DODE-1-B	12	95	5	28.92	19.00	239.5	245.0	2.3
DODE-2-B	12	95	3.4	28.92	27.94	151.3	138.9	8.2
DODE-3-B	12	95	3.29	28.92	28.88	145.7	132.1	9.3
HEXA-1-B	16	60	4	28.92	15.00	136.8	132.5	3.2
HEXA-2-B	16	60	2.1	28.92	28.57	64.7	58.8	9.1
HEXA-3-B	16	60	2.5	28.92	24.00	78.8	74.0	6.1
HEXA-4-B	16	60	2.8	28.92	21.43	89.7	86.5	3.7
HEXA-5-B	16	60	3	28.92	20.00	97.2	94.3	3.0

Table 5: Geometric Properties of Non-compact Sections and FEM results

Specimen	n	b (mm)	t (mm)	λ'	λr	b/t	M_{AASHTO} (KN-m)	M_{FEM} (KN-m)	% Difference
OCT-1-B-N	8	100	2.9	28.92	39.5	34.48	57.5	56.5	1.8
OCT-2-B-N	8	100	2.6	28.92	39.5	38.46	43.6	47.8	9.5
OCT-3-B-N	8	100	2.54	28.92	39.5	39.37	45.9	46.6	1.5
DODE-1-B-N	12	95	3	28.92	36.41	31.67	121.0	119.9	0.9
DODE-2-B-N	12	95	2.61	28.92	36.41	36.4	89.2	93.7	5.0
DODE-3-B-N	12	95	2.8	28.92	36.41	33.93	104.6	103.9	0.6
HEXA-1-B-N	16	60	2	28.92	32.53	30	56.9	54.9	3.5
HEXA-2-B-N	16	60	2.07	28.92	32.53	28.99	62.7	58.0	7.5
HEXA-3-B-N	16	60	1.85	28.92	32.53	32.43	44.6	48.7	9.1

Figure 4 and Figure 5 shows the failure of sections due to local buckling under axial compression and pure bending respectively.

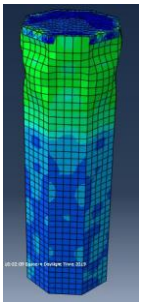

Figure 4: Failure Mode of Model under axial compression

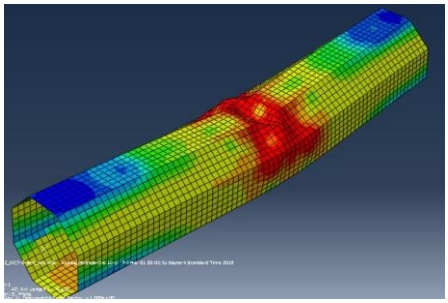

Figure 5: Failure mode of Model under bending

5 DISCUSSION ON FEM RESULTS

5.1 Effect of Plate Width-Thickness Ratio

Plate width-thickness ratio plays a vital role in local buckling capacity. Figure 6 shows the effect of plate width-thickness ratio (b/t) on the buckling capacity of sections under axial compression of this study. To investigate the effect of parameter b/t ratio, a wide range of b/t has been selected. F_{cr} has been divided by corresponding F_y to convert into a dimensionless term. Figure 6 shows the relationship between buckling capacity and plate width-thickness ratio. As expected, with an increase in the width-thickness ratio, the buckling capacity of the axially loaded multisided tube decreases.

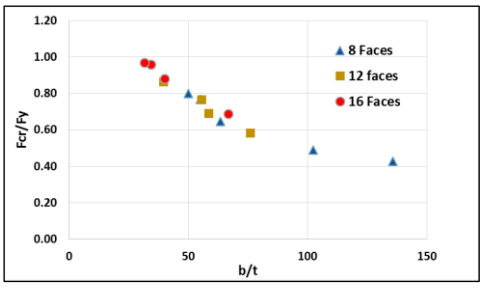

Figure 6: Effect of Plate Width-Thickness Ratio

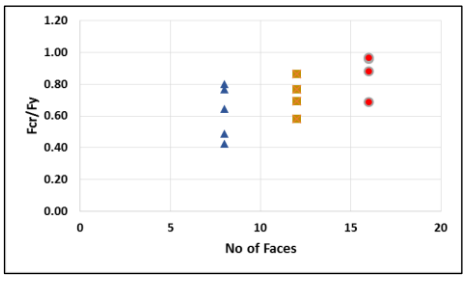

Figure 7: Effect of Number of Faces

5.2 Effect of Number of Faces

Figure 7 shows the variation of buckling capacity with the number of the faces of multisided steel tubular

sections under axial compression. Though DODE-2 and HEXA-3 have a similar plate width-thickness ratio, but different cross-sections. It has been observed that HEXA-3 has nearly 2% more critical buckling stress as compared to DODE-2. Moreover, HEXA-4 has more b/t ratio than OCTA-3. But it has been found that HEXA-4 has 6.7% more critical buckling stress than OCTA-3. Thus, FEM results indicate that local buckling capacity increases with an increase in number of faces.

6 COMPARISON WITH CODES

Both the results of compression tests and bending tests have been compared with codes to see the compatibility of FE results with Codes.

6.1 Multisided Tubes under Compression

Eurocode 3 (EN 1-1, 2005, EN 1-3, 2006, EN 1-5, 2006) has design equation for plate elements. Multisided steel tubular section has been considered as a collection of individual longitudinal plate strip to find the resistance using Eurocode 3. Design equation of EC is based on the effective area concept. According to Eurocode, the effective area can be found from Equation 3, Equation 4 and Equation 5.

[3] $\mathrm{Aeff} = \rho \mathrm{Ag}$

[4] $\rho = \begin{cases} 1, & \lambda p \le 0.5 + \sqrt{(0.085 - 0.055\psi)} \\ \frac{\lambda p - 0.055(3+\psi)}{\lambda p \hat{} 2} \le 1, & \lambda p > 0.5 + \sqrt{(0.085 - 0.055\psi)} \end{cases}$

where ψ= Stress ratio and λp = plate width-thickness parameter

[5] $\lambda p = \sqrt{\frac{Fy}{\sigma cr}}$

σ_{cr}= Elastic critical plate buckling stress from Equation 1

ASCE relies on the effective stress concept supported by the total cross section. Its equations depend on the number of faces (ASCE/SEI-48-11 2011).

Table 6: ASCE Design Equations for Local Buckling Capacity of Multisided Tubular Column

No of Faces	Bend Angle (Degree)	Limit	Compressive Resistance Permitted
4,6 or 8	≥45	$b/t \le 260\Omega/\sqrt{Fy}$	$Fa = Fy$
		$260\Omega/\sqrt{Fy} < b/t \le 351\Omega/\sqrt{Fy}$	$Fa = 1.42Fy(1 - 0.00114\frac{1}{\Omega}\sqrt{Fy}\frac{b}{t})$
		$b/t > 351\Omega/\sqrt{Fy}$	$Fa = 104980\phi/\left(\frac{b}{t}\right)^2$
12	30	$b/t \le 240\Omega/\sqrt{Fy}$	$Fa = 1.45Fy(1 - 0.00129\frac{1}{\Omega}\sqrt{Fy}\frac{b}{t})$
		$240\Omega/\sqrt{Fy} < b/t \le 374\Omega/\sqrt{Fy}$	$Fa = Fy$
		$b/t > 374\Omega/\sqrt{Fy}$	$Fa = 104980\phi/\left(\frac{b}{t}\right)^2$
16	22.5	$b/t \le 215\Omega/\sqrt{Fy}$	$Fa = Fy$
		$215\Omega/\sqrt{Fy} < b/t \le 412\Omega/\sqrt{Fy}$	$Fa = 1.42Fy(1 - 0.00137\frac{1}{\Omega}\sqrt{Fy}\frac{b}{t})$
		$b/t > 412\Omega/\sqrt{Fy}$	$Fa = 104980\phi/\left(\frac{b}{t}\right)^2$

where b= width of one side, Fa is compressive stress permitted, ϕ=6.9 and Ω= 2.62 for Fy and Fa in MPa

To make a homogenous comparison between FEM results and Codes, $\frac{b\sqrt{Fy}}{t}$ of ASCE equations can be converted to 850λp, which is found using equation 1 and equation 5 for E=200GPa.

According to AASHTO, compressive strength of multisided tubular column shall be calculated using Equation 6 to Equation 9 (AASHTO 2015).

[6] $Pnc = AgFcr$

when $\frac{KL}{r} \leq 4.71\sqrt{\frac{E}{QFy}}$

[7] $Fcr = Q(0.658)^{(\frac{QFy}{Fe})}Fy$

when $\frac{KL}{r} > 4.71\sqrt{\frac{E}{QFy}}$

[8] $Fcr = 0.877Fe$, Where $Fe = \pi^2E/(KL/r)^2$

If $\lambda \leq \lambda_r$, Q=1

If $\lambda > \lambda_r$, $Q=A_{EFF}/A_g$, where, A_{EFF} is calculated from the sum of parts using effective widths, be

[9] $be = 1.92t\sqrt{\frac{E}{f}}[1 - \frac{0.34}{\frac{b}{t}}\sqrt{\frac{E}{f}}] \leq b$

where f = F_{cr} using Q=1

Design equations of EC and ASCE are plotted in the graph against plate width-thickness parameter λp in Figure 8. To get a dimensionless quantity, critical buckling stress has been divided by yield stress to plot in the comparison graph.

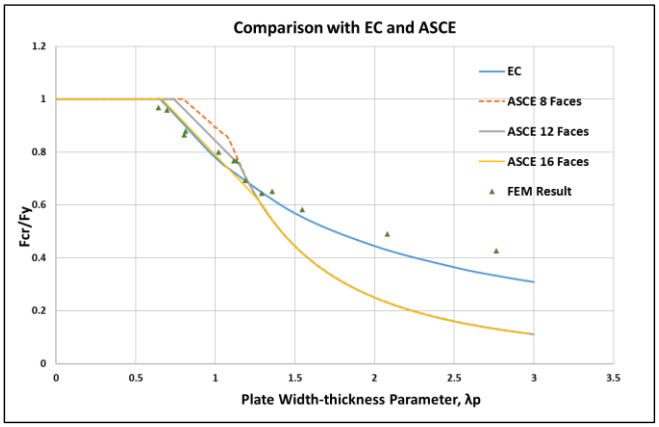

Figure 8: Comparison of FEM results with Eurocode and ASCE

Comparison between FEM results and ASCE shows that for eight faces, ASCE is overestimating the capacity for plate width-thickness parameter (λp) below 1.02 and underestimating for λp more than 2.0. However, for eight faces, ASCE and FEM show good agreement at λp around 1.12 and 1.3. Again for twelve faces, ASCE is overestimating the capacity for λp value of 0.8 and underestimating for λp value of 1.55 as compared to FEM results. ASCE and FEM show good agreement for twelve faces sections having λp between 1.13 and 1.2. Figure 8 shows that ASCE and FEM results are close for λp value below 0.81 for sixteen faces. However, ASCE is estimating a very low capacity for λp value of 1.36 as compared to FEM

results for sixteen faces. FEM result shows good agreement with EC for λp value between 0.64 and 1.6. However, FEM result shows higher capacity for λp value more than 2.

For AASHTO critical loads were calculated using given Equations 6 to Equation 9 and then plotted against the corresponding value of b/t in Figure 9. It is observed that Fcr/Fu for FEM and AASHTO are pretty close for b/t ratio less than 80.

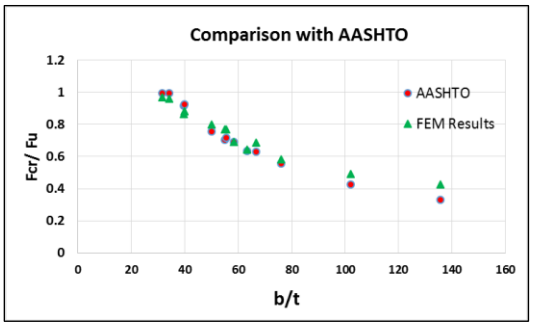

Figure 9: Comparison between FEM Results and AASHTO

6.2 Bending of Compact and Non-compact Sections

According to AASHTO, a compact multisided tubular section would reach plastic moment. From Figure 10, it is observed that most of the compact sections couldn't reach plastic moment. However, the ratios of M_{FEA}/M_{AASHTO} are close to 1, which indicates a good agreement with AASHTO.

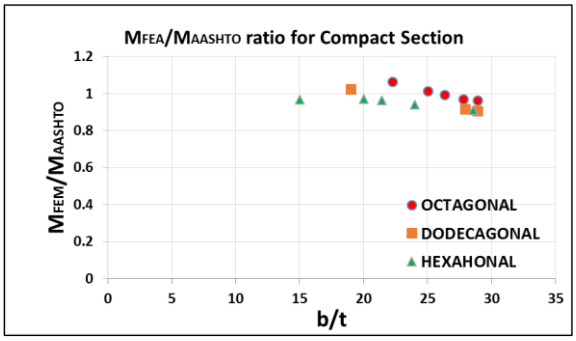

Figure 10: M_{FEA}/M_{AASHTO} ratio for Compact Section

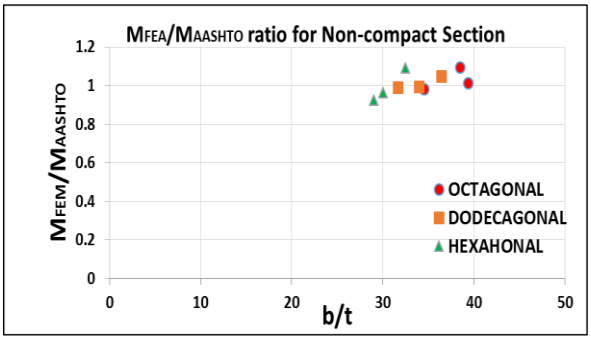

Figure 11: M_{FEA}/M_{AASHTO} ratio for Non-compact Section

Figure 11 shows that two Octagonal, one Dodecagonal and one Hexadecagonal non-compact section could reach the moment capacity indicated by AASHTO. However, for the remaining non-compact sections ratio of bending strength is close to 1. Since all the ratios of M_{FEA}/M_{AASHTO} are close to 1, it indicates good agreement of FEM results with AASHTO.

7 CONCLUSION

This paper presents a finite element (FE) analysis based study of local buckling of multisided steel tubular sections. Nonlinear finite element model has been developed to analyze a series of multisided steel tubular sections under compression and pure bending. Three different geometry, namely, eight, twelve and sixteen sided polygonal sections, are considered. Both linear buckling and nonlinear static analyses are conducted using ABAQUS. A parametric study was conducted to investigate the effect of width-thickness ratio and the number of faces on local buckling capacity. FEM results indicated an increase in local buckling capacity with an increase in number of faces. However, this increase is not that significant. FE results for multisided tube under compression have been compared with EC, AASHTO, and ASCE. ASCE provides different design equations depending on number of faces of the section. ASCE shows agreement with FEM results

for some of the sections. However, for other sections, ASCE is either overestimating or underestimating the buckling capacity as compared to FEM results. ASCE provides smaller buckling capacity for all the sections having λp more than 1.36 as compared to EC and FEM results. FEM result shows good agreement with EC for λp value between 0.64 and 1.6. However, FEM result shows higher capacity for λp value more than 2. AASHTO and FEM results are pretty close for b/t ratio less than 80. Effect of bending on compact and non-compact sections has been studied by developing Finite Element Models. FEM results show that the ratio of bending strength from FE analysis and AASHTO is close to 1 for all the Octagonal, Dodecagonal and Hexadecagonal compact and non-compact sections, indicating good agreement with AASHTO.

ACKNOWLEDGEMENTS

Funding for this research project is provided by the Faculty of Engineering and Computer Science, Concordia University, Montreal, Canada and the Natural Sciences and Engineering Research Council of Canada.

REFERENCES

ABAQUS. 2014. ABAQUS standard user's manual, 6.14. Dassault Systèmes.

American Association of State Highway and Transportation Officials (AASHTO). 2015. LRFD Specifications for Structural Supports for Highway Signs, Luminaires, and Traffic Signals, Washington, DC.

American Society of Civil Engineers (ASCE). 2006. Design of Steel Transmission Pole Structures, ASCE/SEI 48-05, Reston, Virginia.

American Society of Civil Engineers (ASCE). 2011. Design of Steel Transmission Pole Structures, ASCE/SEI 48-11, Reston, Virginia.

Aoki, T., Migita, Y. and Fukumoto, Y. 1991. Local Buckling Strength of Closed Polygon Folded Section Columns. Journal of Constructional Steel Research, **20** (4): 259–270.

Eurocode 3. 2005. *EN 1993-1-1 Eurocode 3: Design of steel structures - Part 1–1: general rules and rules for buildings*. European Committee for Standardization (CEN), Brussels, Belgium.

Eurocode 3. 2006. *EN 1993-1-3 Eurocode 3: Design of steel structures - Part 1–3:* General rules-Supplementary rules for cold-formed members and sheeting. European Committee for Standardization (CEN), Brussels, Belgium.

Eurocode 3. 2006. *EN 1993-1-5 Eurocode 3: Design of steel structures - Part 1–5:* General rules - Plated structural elements. European Committee for Standardization (CEN), Brussels, Belgium.

Godat, A., Legeron, F., Bazonga, D. 2012. Stability Investigation of Local Buckling Behavior of Tubular Polygon Columns under Concentric Compression. Thin-Walled Structures, **53**:131-140.

Migita, Y. and Fukumoto, Y. 1997. Local Buckling Behaviour of Polygonal Sections. Journal of Constructional Steel Research, **41**(2/3): 221–233.

Teng, J.G., Smith, S.T. and Ngok, L.Y. 1999. Local Buckling Of Thin-Walled Tubular Polygon Columns Subjected To Axial Compression or Bending. Proceedings of the Second International Conference on Advances in Steel Structures, Elsevier Steel Structures Division, Hong Kong, China, **1**:109–115.

Timoshenko, S.P. and Gere J.M. 1961.Theory of Elastic Stability. 2nd ed., McGraw Hill, New York, NY, USA.

Trahair, N. S. 1993. Flexural-Torsional buckling of structures. *CRC Press*, Boca Raton, FL.